



## Research Article

# Biparametric versus multiparametric magnetic resonance imaging of the prostate: detection of clinically significant cancer in a perfect match group



Junghyeum Cho <sup>a</sup>, Hyungwoo Ahn <sup>a</sup>, Sung Il Hwang <sup>a, \*</sup>, Hak Jong Lee <sup>a</sup>, Gheeyoung Choe <sup>b</sup>, Seok-Soo Byun <sup>c</sup>, Sung Kyu Hong <sup>c</sup>

<sup>a</sup> Department of Radiology, Seoul National University Bundang Hospital, Seongnam-si, Gyeonggi-do, Korea

<sup>b</sup> Department of Pathology, Seoul National University Bundang Hospital, Seongnam-si, Gyeonggi-do, Korea

<sup>c</sup> Department of Urology, Seoul National University Bundang Hospital, Seongnam-si, Gyeonggi-do, Korea

## ARTICLE INFO

## Article history:

Received 1 October 2019

Received in revised form

12 December 2019

Accepted 28 December 2019

Available online 26 February 2020

## Keywords:

Biparametric

Magnetic resonance imaging

Multiparametric

Prostate cancer

Prostate imaging reporting and data system

## ABSTRACT

**Background:** Biparametric (bp) magnetic resonance imaging (MRI) could be an alternative MRI for the detection of the clinically significant prostate cancer (csPCa).

**Purpose:** To compare the accuracies of prostate cancer detection and localization between prebiopsy bpMRI and postbiopsy multiparametric MRI (mpMRI) taken on different days, using radical prostatectomy specimens as the reference standards.

**Material and methods:** Data of 41 total consecutive patients who underwent the following examinations and procedures between September 2015 and March 2017 were collected: (1) magnetic resonance—and/or ultrasonography-guided biopsy after bpMRI; (2) postbiopsy mpMRI; and (3) radical prostatectomy with csPCa. Two radiologists scored suspected lesions on bpMRI and mpMRI independently using Prostate Imaging Reporting and Data System version 2. The diagnostic accuracy of detecting csPCa and the Dice similarity coefficient were obtained. Apparent diffusion coefficient (ADC) ratios were also obtained for quantitative comparison between bpMRI and mpMRI.

**Results:** Diagnostic accuracies on bpMRI and mpMRI were 0.83 and 0.82 for reader 1; 0.80 and 0.82 for reader 2. There are no significantly different values of diagnostic sensitivities or specificities between the readers or between MRI protocols. Intra-observer Dice similarity coefficient was significantly lower in reader 2, compared to that in reader 1 between the two MRI protocols. The range of mean ADC ratio was 0.281–0.635. There was no statistically significant difference in the ADC ratio between bpMRI and mpMRI.

**Conclusions:** Diagnostic performance of bpMRI without dynamic contrast enhancement MRI is not significantly different from mpMRI with dynamic contrast enhancement MRI in the detection of csPCa.

© 2020 Asian Pacific Prostate Society, Published by Elsevier Korea LLC. This is an open access article under the CC BY-NC-ND license (<http://creativecommons.org/licenses/by-nc-nd/4.0/>).

## 1. Introduction

Prostate cancer has been the most common malignancy for decades and is the second leading cause of cancer-related death of men in the United States<sup>1</sup>. Diagnosis of prostate cancer is traditionally performed by monitoring the elevated prostate-specific antigen (PSA) level, rectal examination tests, and subsequent

histological examination such as ultrasonography-guided biopsy. Magnetic resonance imaging (MRI) helps to localize, determine the stage, and predict the aggressiveness of the prostate cancer<sup>2–4</sup>. Multiparametric (mp) prostate MRI, which is recommended by current guidelines of Prostate Imaging Reporting and Data System version 2 (PI-RADSv2), includes multiplanar T1-weighted (T1W) and T2-weighted (T2W) imaging as well as functional sequence diffusion-weighted imaging (DWI) and dynamic contrast enhancement (DCE) imaging<sup>5</sup>.

Because of various sequences, mpMRI takes a relatively long time, approximately 30–45 minutes<sup>6</sup>. In addition, the use of gadolinium-based contrast agents presents problems of

\* Corresponding author. Department of Radiology, Seoul National University Bundang Hospital, 300 Gumi-dong, Bundang-gu, Seongnam-si, Gyeonggi-do, 13620, Korea.

E-mail address: [hwangsi49@gmail.com](mailto:hwangsi49@gmail.com) (S.I. Hwang).

inconvenience of intravenous catheterization and the potential risk of several adverse events such as nephrogenic systemic fibrosis or gadolinium deposition in the brain. In PI-RADSv2, unlike in earlier guidelines, the role of DCE-MRI is downgraded and plays only a minor role in tumor assessment (tertiary sequence in the evaluation of the lesions in the peripheral zone [PZ] and no role in the transition zone [TZ]). To overcome these drawbacks, biparametric (bp) prostate MRI (only T2W imaging and DWI) is considered to be an alternative for the detection and evaluation of prostate cancer; several studies have reported promising results<sup>7,8</sup>. However, most studies comparing the diagnostic performance of mpMRI and bpMRI used a fraction of mpMRI sequences to make up bpMRI and were reported based on biopsy specimens, causing controversial results<sup>6,9-12</sup>. Therefore, the purpose of this study is to compare prostate cancer detection and localization accuracy of prebiopsy bpMRI and postbiopsy mpMRI taken on different days, using radical prostatectomy specimens as the reference standard.

**2. Materials and Methods**

Our study was retrospectively conducted in a single center, tertiary referral hospital. The institutional review board approved this study and waived the requirement for informed consent (B-1708-412-134).

**2.1. Study Population**

Among the consecutive patients who underwent bpMRI between September 2015 and March 2017, data of patients who underwent the following examinations and procedures were collected: (1) magnetic resonance (MR)- and/or ultrasonography-guided biopsy after bpMRI; (2) postbiopsy mpMRI; and (3) radical prostatectomy with histopathologically confirmed, clinically significant prostate cancer (csPCa), which was defined as Gleason score (GS)  $\geq 7$  cancer or GS 6 cancer with more than 0.5 cm<sup>3</sup> volume<sup>13,14</sup>. Finally, 41 patients with a mean age  $\pm$  standard deviation (SD) of 64.3  $\pm$  6.2 years (range 51–75 years) constituted the authors study population (Fig. 1). Selected patients did not have histories of previous biopsies or any other surgeries, such as transurethral resection. The mean interval  $\pm$  SD between bpMRI and mpMRI was 35  $\pm$  24 days (range 8–157 days); the mean interval  $\pm$  SD between mpMRI and radical prostatectomy was 9.9  $\pm$  9.7 days (range 0–47 days) (Table 1).

**2.2. MR Protocol**

Patients were scanned with 3.0-T Ingenia or 3.0-T Achieva Tx MR units (Philips Healthcare, Best, the Netherlands). Antiperistaltic drugs (Buscopan, Boehringer Ingelheim, Germany) were injected

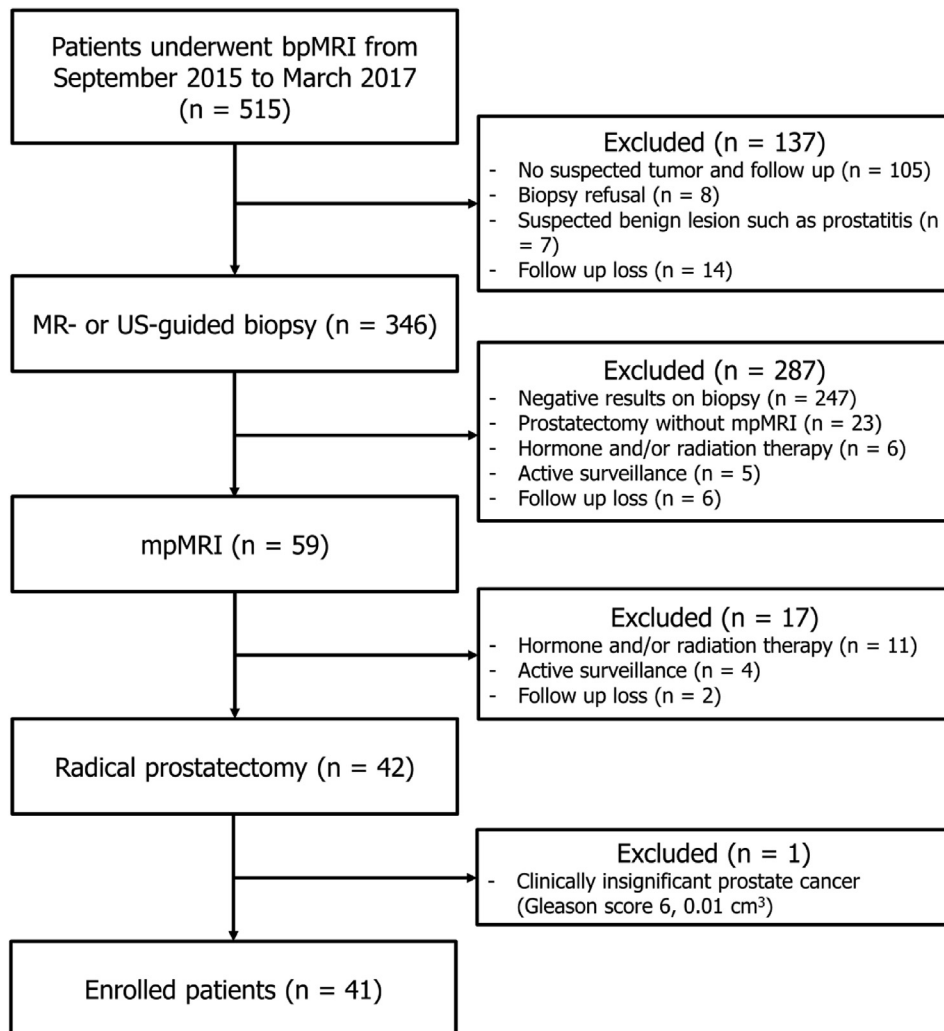


**Fig. 1.** Flow chart of patient inclusion. bpMRI, biparametric magnetic resonance imaging; mpMRI, multiparametric MRI; MR, magnetic resonance; US, ultrasonography.

**Table 1**  
Clinical–pathologic features in the study population (n = 41).

Age (yr)	
Mean	64.3 ± 6.12
Range	51–75
Serum PSA level (ng/mL)	
Mean	9.2 ± 5.3
Range	2.9–22.9
Prostate volume (mL)	
Mean	33.1 ± 11.4
Range	15.9–69.0
PSA density (ng/mL <sup>2</sup> )	
Mean	0.31 ± 0.25
Range	0.10–1.44
Diameter of index lesion (cm)	
Mean	1.9 ± 0.8
Range	0.4–3.9
ISUP 2014 grading <sup>a</sup>	
1	10 (24)
2	18 (44)
3	9 (22)
4	3 (7)
5	1 (2)
Pathologic tumor staging <sup>a</sup>	
T2a	2 (5)
T2c	31 (76)
T3a	8 (20)

PSA, prostate-specific antigen; ISUP, International Society of Urological Pathology.

<sup>a</sup> Data are numbers of patients, with percentages in parentheses. Percentages may not add up to 100% because of rounding.

intramuscularly 30 minutes before the MR examination. The protocol and the pulse sequence parameters used in bpMRI and mpMRI followed the technical recommendations suggested by current guidelines (PI-RADSv2)<sup>5</sup>, as summarized in Table 2.

In bpMRI, T1W and T2W fast spin-echo images were obtained in the transverse plane without fat suppression covering the prostate gland and the seminal vesicles. In mpMRI, T2W fast spin-echo images with additional planes (sagittal without fat suppression and coronal with fat suppression) were acquired, covering the prostate gland and the seminal vesicles. In both protocols, DWI was obtained in the transverse plane with the same orientation as was used for the T2W images. Apparent diffusion coefficient (ADC) parametric maps were calculated using a monoexponential fit based on three b values (0, 100, and 1000 s/mm<sup>2</sup>).

In the mpMRI, DCE images were obtained in transverse sections using a three-dimensional T1W gradient-echo sequence with fat-suppression technique (THRIVE) sequence with a temporal resolution of 5 seconds. Gadobutrol (Gadovist; Bayer Schering Pharma, Berlin, Germany) was used as a contrast agent in a dose of 0.1 mmol/kg of body weight with a flow rate of 2 mL/s.

### 2.3. Image Analysis

Two radiologists—with 15 (reader 1, an expert) and 3 years (reader 2, a resident) of experience in prostate MRI, respectively—reviewed the bpMRI and mpMRI independently, localizing

and evaluating suspicious lesions using PI-RADSv2. They were informed that all the patients had undergone radical prostatectomies and had csPCa. However, the radiologists were unaware of the patients' clinical (rectal examination), biological (serum PSA level), and histopathological results (location, stage, or GS). For reporting, the prostate was subdivided into 12 segments: four quadrants (anterior right, anterior left, posterior right, and posterior left) in the transverse plane and three levels (base, mid, and apex) in the craniocaudal direction. The urethra was adopted as an anatomic reference, dividing the anterior and posterior sectors.

The likelihood of prostate cancer was assessed using PI-RADSv2 assessment categories<sup>5</sup>; all the detected lesions were classified as categories 1–5. For lesions of TZ, the category was mainly determined by the T2W image; category 3 on the T2W image was upgraded to category 4 when the lesion was classified as category 5 on the DWI. For lesions of PZ, DWI played a key role; when DCE was positive on the mpMRI, category 3 lesions on the DWI were upgraded to category 4. On the bpMRI, DCE measurement was unavailable; in case of DWI category 3 lesion in PZ, T2W image used instead, with threshold ≥ category 4 considered positive, resulting in upgrade of overall assessment categories 3–4<sup>15</sup>. Categories 1–3 were considered negative, whereas categories 4 and 5 were considered positive. The greatest dimension of categories 4 and 5 lesions was measured for comparison with prostatectomy specimens.

The postbiopsy hemorrhage amount on the mpMRI was also assessed for evaluation of influence on diagnostic performance. Hemorrhages usually appear as hypointensity on the T2W image, which may look similar to typical prostate cancer. However, comparing the hyperintensity seen on the T1W image may be helpful in locating the tumor<sup>16</sup>. To evaluate the effect of hemorrhage seen on postbiopsy mpMRI, a positive result was defined when hemorrhages were more than half of each segment; radiologists reported the number of positive segments: 1–3 (0–25%) as 1, 4–6 (25–50%) as 2, 7–9 (50–75%) as 3, and 10–12 (75–100%) as 4, respectively.

### 2.4. Matching of MRI and Prostatectomy Specimen

Clinically significant prostate cancer in the radical prostatectomy specimen was analyzed using the formal pathologic maps and report, which contained information about the location, size, and Gleason's score of the tumor. Localization was reported as 12 segments and the zonal anatomy of the prostate. Segment-based diagnostic performance, including sensitivity, specificity, positive predictive value (PPV), and negative predictive value (NPV), was obtained based on the reports by the two radiologists compared with the pathologic reports. In addition, a patient-based agreement between MR-specified lesions and csPCa in the prostatectomy specimen was determined by a consensus of two readers using the pathologic map. Correlation of prostate MRI to histopathologic maps is known to be difficult<sup>17</sup>.

**Table 2**  
MRI protocols.

MRI	Sequence	View	TR (ms)	TE (ms)	FOV (mm × mm)	Matrix	Slice thickness (mm)	Interslice gap (mm)	NSA	Scan time (min:s)	Temporal resolution (s)
BP & MP	T2W	Axial	2,789	90	150 × 150	300 × 298	3	1	1	3:04	
	DW (b = 0, 100, 1000)	Axial	5,975	55	224 × 224	112 × 111	3	0	1	3:17	
	T1W	Axial	554	10	150 × 150	300 × 300	3	1	1	3:22	
MP only <sup>a</sup>	DCE	Axial	4	1.5	160 × 160	108 × 105	8	–4	2	5:02	5

BP, biparametric; DCE, dynamic contrast enhancement; DW, diffusion-weighted; MP, multiparametric; MRI, magnetic resonance imaging; SPIR, Spectral Presaturation with Inversion Recovery; T1W, T1-weighted; T2W, T2-weighted; TR, repetition time; TE, echo time; FOV, field of view; NSA, number of signals averaged.

<sup>a</sup> MP also included T2W sagittal image, T2W SPIR coronal image, and T1W SPIR contrast enhanced axial image.

### 2.5. ADC Value Analysis

After matching the MRI and prostatectomy maps, one radiologist located tumors on an ADC map using commercial analysis software (Intellispace Portal version 9.0.1; Philips Healthcare, Best, the Netherlands). Anatomical landmark structures such as the border between the TZ and PZ, verumontanum, urethra, and other benign lesions including cysts, calcification, and hyperplastic nodules<sup>2,18</sup> were used to help precise localization. Regions of interest (ROIs) were drawn carefully for tumors, which appeared as lesions with focal hyperintensity on high b-value ( $b = 1000 \text{ s/mm}^2$ ), DWI, and corresponding low focal ADC value, relative to surrounding benign tissues.

For the visible lesion, the ROI was measured as large as possible on the slice showing the maximum width of the tumor; the tumor edge was not included<sup>19</sup>. For the invisible lesion, the histopathologic map and anatomical structure were used as a reference, and the ROI was drawn at the corresponding tumor location on the ADC map. To minimize mismatch between the ADC and histopathologic maps, the tumor ROI on the ADC was drawn smaller than size on the histopathologic map<sup>18</sup>. In addition, ROIs of at least  $20 \text{ mm}^2$  were drawn on the homogeneous portion of the PZ, TZ, and urinary bladder without tumors, as previous reports suggested<sup>2,20,21</sup>. The ADC ratio was calculated by dividing the ADC value of the tumor by the reference ADC value. A total of four ADC ratios were obtained according to the reference zone: tumor-to-PZ, tumor-to-TZ, tumor-to-tumor zone (same value as tumor-to-PZ or tumor-to-TZ depending on tumor location), and tumor-to-urinary bladder<sup>2,20</sup>.

### 2.6. Statistical Analysis

Statistical analysis was performed using SPSS version 19.0 software (IBM, Armonk, NY). A  $P$  value  $< 0.05$  was considered to be statistically significant. Diagnostic performance, including sensitivity, specificity, PPV, NPV, and accuracy was compared between the two readers using McNemar tests. The Dice similarity coefficient (DSC) was calculated to quantify spatial agreements of suspected lesions between the readers and between the two MRI protocols; DSCs were also compared using the independent samples Student  $t$  test. The greatest dimensions of PI-RADS 4 and 5 lesions were compared between bpMRI and mpMRI by using Wilcoxon signed rank tests. Also, weighted Cohen kappa was used to evaluate the degree of inter-observer agreement in postbiopsy hemorrhage. The ADC ratios of the bpMRI and mpMRI were compared using the independent samples Student  $t$  test.

## 3. Results

### 3.1. Patient and Tumor Characteristics

The mean preoperative serum PSA level of the 41 patients was  $9.2 \pm 5.3 \text{ ng/mL}$  (range 2.9–22.9 ng/mL). Pathologic stages were IIa ( $n = 1$ ), IIc ( $n = 31$ ), and IIIa ( $n = 9$ ). Gleason scores based on biopsy were 6 in 10 (24.4%), 7 (3 + 4) in 18 (43.9%), 7 (4 + 3) in 9 (22.0%), 8 in 3 (7.3%), and 9 in 1 (2.4%) patients, respectively. The mean percentage of positive cores was  $23.4 \pm 12.7\%$  (range 0–58.3%) on routine transrectal 12-core biopsy. A total of 85 combined MR/US-guided target biopsies for suspicious tumors were performed in 39 patients, and 49 positive cores (55.1%) were obtained.

Gleason scores of prostatectomy specimens were 7 (3 + 4) in 27 (65.9%), 7 (4 + 3) in 11 (26.8%), and 9 in 3 (7.3%) patients, respectively. Regarding extraprostatic disease, 8 patients (19.5%) had an extracapsular extension, and none had a seminal vesical invasion. Among 26 patients who underwent lymph node dissection, none had lymph node metastasis. Mean prostate volume and tumor

volume percentage based on radical prostatectomy were  $33.1 \pm 11.4 \text{ cm}^3$  (range 15.9–69.0) and  $8.9\% \pm 7.9\%$  (range 1–35%).

### 3.2. Diagnostic Performance

The sensitivities, specificities, PPV, and NPV of localizing csPCa on bpMRI were 0.22, 0.97, 0.63, and 0.85 for reader 1; 0.20, 0.94, 0.41, and 0.84 for reader 2, respectively. These measurements on the mpMRI were 0.22, 0.95, 0.5, and 0.84 for reader 1; 0.24, 0.96, 0.55, 0.85 for reader 2, respectively. Accuracies on the bpMRI and mpMRI were 0.83 and 0.82 for reader 1; 0.80 and 0.82 for reader 2. There were no significantly different diagnostic parameters between the readers or the MRI protocols.

The inter-observer DSC of mean  $\pm$  SD between readers 1 and 2 was  $0.29 \pm 0.42$  for the bpMRI and  $0.46 \pm 0.48$  for the mpMRI ( $p = 0.09$ ). The intra-observer DSC of mean  $\pm$  SD between the bpMRI and the mpMRI was  $0.43 \pm 0.45$  for reader 1 and  $0.20 \pm 0.38$  for reader 2 ( $p = 0.01$ ). The intra-observer DSC was significantly lower in reader 2 compared to reader 1 between the two MRI protocols.

The mean greatest dimension (mean  $\pm$  SD) of PI-RADS categories 4 and 5 on the bpMRI and mpMRI was  $13.6 \pm 5.1 \text{ mm}$  and  $13.6 \pm 5.8 \text{ mm}$  for reader 1;  $15.4 \pm 5.2 \text{ mm}$  and  $13.6 \pm 4.8 \text{ mm}$  for reader 2. The dimension measured by reader 2 on the mpMRI was significantly decreased compared with that on the bpMRI ( $p = 0.025$ ) and similar to those measured by reader 1. Evaluation of the postbiopsy hemorrhage amount showed good inter-observer agreement ( $\kappa = 0.627$ ) between the two readers.

The range of the mean ADC ratio was 0.281–0.635 (Table 3). There was no statistically significant difference in the ADC ratio between the bpMRI and mpMRI.

## 4. Discussion

This study compared the diagnostic performance in detection and localization of csPCa in patients who underwent radical prostatectomy and two preoperative prostate MRIs; bpMRI and mpMRI. Our results support that bpMRI composed of a T2W and DWI sequence is similar in diagnostic performance to mpMRI, which is in agreement with many studies including recent meta-analysis<sup>6,9,13,22–26</sup>. In addition, there was no statistically significant difference in the ADC ratio between the two MRI protocols, which was performed to assess the quantitative difference of MRI.

There was no significant difference in the diagnostic performance of the experienced and inexperienced reader, as Di Campi et al<sup>27</sup> suggested. However, for reader 2, intra-observer DSC

**Table 3**

Comparison of ADC and ADC ratios between prebiopsy biparametric and postbiopsy multiparametric prostate MRI.

	Biparametric MRI	Multiparametric MRI	$P$
ADC ( $\times 10^{-6} \text{ mm}^2/\text{s}$ )			
Tumor	$760.3 \pm 154.8$	$722.3 \pm 156.0$	0.272
Peripheral zone	$1843.3 \pm 225.9$	$1796.3 \pm 156.4$	0.276
Transition zone	$1199.8 \pm 97.0$	$1223.5 \pm 86.8$	0.246
Tumor zone	$1574.1 \pm 345.7$	$1575.2 \pm 295.6$	0.987
Urinary bladder	$2596.5 \pm 265.3$	$2583.7 \pm 246.8$	0.821
ADC ratio			
Tumor-to-peripheral zone	$0.42 \pm 0.09$	$0.40 \pm 0.08$	0.512
Tumor-to-transition zone	$0.64 \pm 0.12$	$0.59 \pm 0.14$	0.148
Tumor-to-tumor zone	$0.51 \pm 0.15$	$0.48 \pm 0.15$	0.414
Tumor-to-urinary bladder	$0.29 \pm 0.06$	$0.28 \pm 0.06$	0.336

Data are mean  $\pm$  SD, and  $P$  values were calculated using the unpaired  $t$  test. ADC, apparent diffusion coefficient; MRI, magnetic resonance imaging; SD, standard deviation.

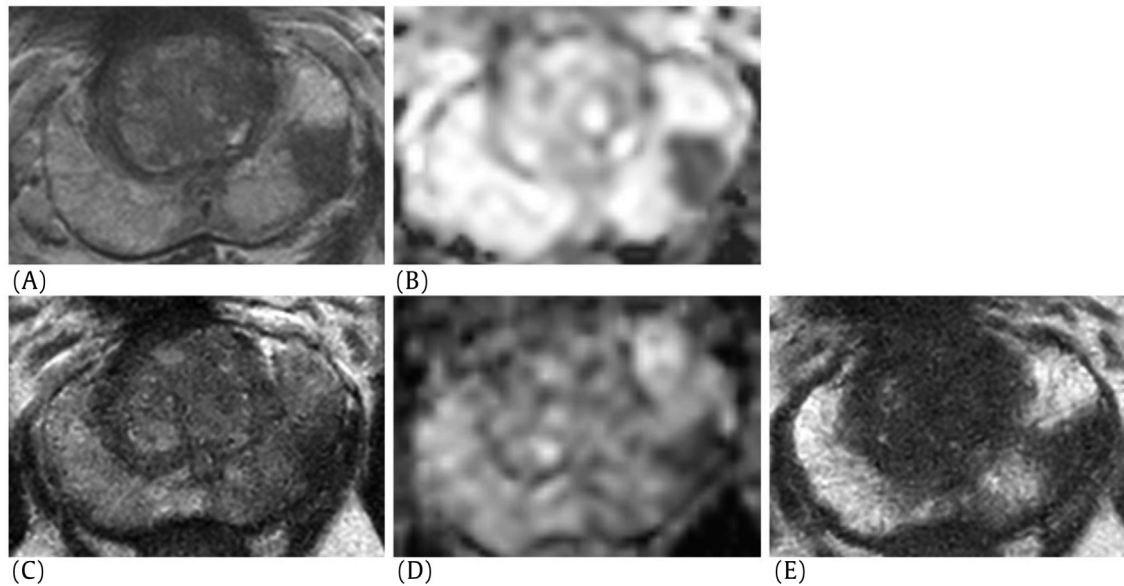


**Fig. 2.** A 58-year-old biopsy-naïve man with prostate cancer in left peripheral zone (GS 4 + 5 = 9 on prostatectomy specimen; PSA level, 14.7 ng/mL). Prebiopsy T2W image (A) and ADC map (B) show a hypointense lesion in the left peripheral zone of the midgland, which appears less prominent on postbiopsy T2W (C) and ADC map (D). Postbiopsy T1W image (E) shows diffuse hemorrhage in the peripheral zone. ADC, apparent diffusion coefficient; GS, Gleason score; PSA, prostate-specific antigen; T1W, T1-weighted; T2W, T2-weighted.

between bpMRI and mpMRI was significantly lower than that in reader 1, and the mean measured the greatest diameter of the suspected lesion was larger on bpMRI than that on mpMRI. These results might be attributed to the fact that postbiopsy hemorrhage from the mpMRI affected the lesion conspicuity on ADC image, especially for inexperienced radiologists. The DSC measures the amount of overlap between a pair of regions and ranges from 0 (no overlap) to 1 (complete overlap)<sup>28</sup>, which could express how similar the selected segments are by two readers (inter-observer) and between bpMRI and mpMRI (intra-observer). Lower intra-observer DSC with relative high SD might imply low reproducibility of tumor detection. The mean greatest dimension of PI-RADS categories 4 and 5 lesions on mpMRI measured by reader 2 was similar to that of reader 1. As seen in the previous study<sup>16</sup>, the margin of the suspected lesion on the mpMRI seemed to be attributed clearly to the hemorrhage exclusion sign after biopsy (Fig. 2).

Most previous studies<sup>13,22,24,26,27</sup> that compare the diagnostic performance of bpMRI and mpMRI extracted T2W and DWI sequences retrospectively from mpMRI. On the other hand, this study compared two MRIs taken on different dates and found no difference in diagnostic performance and ADC ratio between bpMRI and mpMRI. This result supports the authors hypothesis that bpMRI is sufficient for detecting csPCa. However, except in csPCa detection, the role of bpMRI for clinical staging is limited and has not been evaluated well except by the preliminary report on bpMRI detection of extraprostatic extension<sup>29</sup>. In addition, the reference standard of the csPCa in this study was a whole-mount prostatectomy specimen. Considering the positive biopsy result of combined MR/US-guided biopsy was 55.1%, correlation with a radical prostatectomy specimen could reduce false positives and false negatives of missed or incorrect targeting on the biopsy.

One patient was upgraded by reader 1 to PI-RADS category 4 with a DCE positive. The patient's csPCa had a volume of 0.42 cm<sup>3</sup> and 7 (3 + 4) of GS as a result of prostatectomy. The DCE sequence on the mpMRI is not only important in upgrading PI-RADS category 3 lesions in PZ to category 4<sup>30</sup> but may also improve diagnostic performance of prostate cancer, particularly in less experienced

residents, by detecting lesions missed on bpMRI<sup>31</sup> and in patient with prostatitis or previous prostate biopsy. However, the overall detection rate of csPCa was not significantly different in this study.

This study has several limitations. First, the study consisted of a relatively small number of patients and had a retrospective design. A prospective study with a large patient sample is warranted. Secondly, the sensitivity of the csPCa detection was 0.20–0.24, which was relatively low. This can be attributed to the relatively low-grade histopathology of prostate cancer; of 41 patients, 28 patients showed GS 6 and 7 (3 + 4) on biopsy, and no patient showed lymph node or other distal metastasis. The accuracy of csPCa detection was 0.80–0.83, which is relatively reasonable. However, because history of radical prostatectomy was part of the inclusion criteria on this study, early stage prostate cancer samples might be not included in this study. Therefore, results should be interpreted with caution for early stage prostate cancer.

In conclusion, for the detection of csPCa, bpMRI showed similar predictive values compared to mpMRI.

### Conflicts of interest

The authors declare that there is no relevant or material financial interests that relate to the research described in this paper.

### Acknowledgments

This work was supported by the Institute for Information & Communications Technology Promotion (IITP) grant funded by the South Korea government (MSIT, No. 2018-0-00861, Intelligent SW Technology Development for Medical Data Analysis).

### References

1. Siegel RL, Miller KD, Jemal A. Cancer statistics. *CA A Cancer J Clin* 2018;68(1): 7–30, 2018.
2. Woo S, Kim SY, Cho JY, Kim SH. Preoperative evaluation of prostate cancer aggressiveness: using ADC and ADC ratio in determining Gleason score. *AJR Am J Roentgenol* 2016;207(1):114–20.

3. Scheenen TW, Rosenkrantz AB, Haider MA, Futterer JJ. Multiparametric magnetic resonance imaging in prostate cancer management: current status and future perspectives. *Invest Radiol* 2015;50(9):594–600.
4. Rosenkrantz AB, Shanbhogue AK, Wang A, Kong MX, Babb JS, Taneja SS. Length of capsular contact for diagnosing extraprostatic extension on prostate MRI: assessment at an optimal threshold. *J Magn Reson Imag: JMRI* 2016;43(4):990–7.
5. Weinreb JC, Barentsz JO, Choyke PL, Cornud F, Haider MA, Macura KJ, et al. PI-RADS prostate imaging - reporting and data system: 2015, version 2. *Eur Urol* 2016;69(1):16–40.
6. Kuhl CK, Bruhn R, Kramer N, Nebelung S, Heidenreich A, Schrading S. Abbreviated biparametric prostate MR imaging in men with elevated prostate-specific antigen. *Radiology* 2017;285(2):493–505.
7. Fascelli M, Rais-Bahrami S, Sankineni S, Brown AM, George AK, Ho R, et al. Combined biparametric prostate magnetic resonance imaging and prostate-specific antigen in the detection of prostate cancer: a validation study in a biopsy-naive patient population. *Urology* 2016;88:125–34.
8. Jambor I, Bostrom PJ, Taimen P, Syvanen K, Kahkonen E, Kallajoki M, et al. Novel biparametric MRI and targeted biopsy improves risk stratification in men with a clinical suspicion of prostate cancer (IMPROD trial). *J Magn Reson Imag: JMRI* 2017;46(4):1089–95.
9. Van Nieuwenhove S, Saussez TP, Thiry S, Trefois P, Annet L, Michoux N, et al. Prospective comparison of a fast 1.5-T biparametric with the 3.0-T multiparametric ESUR magnetic resonance imaging protocol as a triage test for men at risk of prostate cancer. *BJU Int* 2019;123(3):411–20.
10. Obmann VC, Pahwa S, Tabayayong W, Jiang Y, O'Connor G, Dastmalchian S, et al. Diagnostic accuracy of a rapid biparametric MRI protocol for detection of histologically proven prostate cancer. *Urology* 2018;133–8.
11. Kitajima K, Kaji Y, Fukabori Y, Yoshida K, Suganuma N, Sugimura K. Prostate cancer detection with 3 T MRI: comparison of diffusion-weighted imaging and dynamic contrast-enhanced MRI in combination with T2-weighted imaging. *J Magn Reson Imag: JMRI* 2010;31(3):625–31.
12. Iwazawa J, Mitani T, Sassa S, Ohue S. Prostate cancer detection with MRI: is dynamic contrast-enhanced imaging necessary in addition to diffusion-weighted imaging? *Diagn Intervent Radiol(Ankara, Turkey)* 2011;17(3):243–8.
13. Barth BK, De Visschere PJL, Cornelius A, Nicolau C, Vargas HA, Eberli D, et al. Detection of clinically significant prostate cancer: short dual-pulse sequence versus standard multiparametric MR imaging—a multireader study. *Radiology* 2017;284(3):725–36.
14. Matoso A, Epstein JI. Defining clinically significant prostate cancer on the basis of pathological findings. *Histopathology* 2019;74(1):135–45.
15. De Visschere P, Lumen N, Ost P, Decaestecker K, Pattyn E, Villeirs G. Dynamic contrast-enhanced imaging has limited added value over T2-weighted imaging and diffusion-weighted imaging when using PI-RADSV2 for diagnosis of clinically significant prostate cancer in patients with elevated PSA. *Clin Radiol* 2017;72(1):23–32.
16. Barrett T, Vargas HA, Akin O, Goldman DA, Hricak H. Value of the hemorrhage exclusion sign on T1-weighted prostate MR images for the detection of prostate cancer. *Radiology* 2012;263(3):751–7.
17. Hoeks CM, Hambroek T, Yakar D, Hulsbergen-van de Kaa CA, Feuth T, Witjes JA, et al. Transition zone prostate cancer: detection and localization with 3-T multiparametric MR imaging. *Radiology* 2013;266(1):207–17.
18. Kim CK, Park SY, Park JJ, Park BK. Diffusion-weighted MRI as a predictor of extracapsular extension in prostate cancer. *AJR Am J Roentgenol* 2014;202(3):W270–6.
19. Boesen L, Chabanova E, Logager V, Balslev I, Thomsen HS. Apparent diffusion coefficient ratio correlates significantly with prostate cancer gleason score at final pathology. *J Magn Reson Imag: JMRI* 2015;42(2):446–53.
20. De Cobelli F, Ravelli S, Esposito A, Giganti F, Gallina A, Montorsi F, et al. Apparent diffusion coefficient value and ratio as noninvasive potential biomarkers to predict prostate cancer grading: comparison with prostate biopsy and radical prostatectomy specimen. *AJR Am J Roentgenol* 2015;204(3):550–7.
21. Lebovici A, Sfrangeu SA, Feier D, Caraianni C, Lucan C, Suciuc M, et al. Evaluation of the normal-to-diseased apparent diffusion coefficient ratio as an indicator of prostate cancer aggressiveness. *BMC Med Imag* 2014;14:15.
22. Scialpi M, Prosperi E, D'Andrea A, Martorana E, Malaspina C, Palumbo B, et al. Biparametric versus multiparametric MRI with non-endorectal coil at 3T in the detection and localization of prostate cancer. *Anticancer Res* 2017;37(3):1263–71.
23. Kang Z, Min X, Weinreb J, Li Q, Feng Z, Wang L. Abbreviated biparametric versus standard multiparametric MRI for diagnosis of prostate cancer: a systematic review and meta-analysis. *AJR Am J Roentgenol* 2018;W1–9.
24. Sherrer RL, Glaser ZA, Gordetsky JB, Nix JW, Porter KK, Rais-Bahrami S. Comparison of biparametric MRI to full multiparametric MRI for detection of clinically significant prostate cancer. *Prostate Cancer Prostatic Dis* 2019;22(2):331–6.
25. Woo S, Suh CH, Kim SY, Cho JY, Kim SH, Moon MH. Head-to-Head comparison between biparametric and multiparametric MRI for the diagnosis of prostate cancer: a systematic review and meta-analysis. *AJR Am J Roentgenol* 2018;211(5):W226–41.
26. Junker D, Steinkohl F, Fritz V, Bektic J, Tokas T, Aigner F, et al. Comparison of multiparametric and biparametric MRI of the prostate: are gadolinium-based contrast agents needed for routine examinations? *World J Urol* 2018;37(4):691–9.
27. Di Campli E, Delli Pizzi A, Seccia B, Cianci R, d'Annibale M, Colasante A, et al. Diagnostic accuracy of biparametric vs multiparametric MRI in clinically significant prostate cancer: comparison between readers with different experience. *Eur J Radiol* 2018;101:17–23.
28. Dice LR. Measures of the amount of ecologic association between species. *Ecology* 1945;26(3):297–302.
29. Stanzione A, Cuocolo R, Coccozza S, Romeo V, Persico F, Fusco F, et al. Detection of Extraprostatic Extension of Cancer on Biparametric MRI Combining Texture Analysis and Machine Learning: Preliminary Results. *Acad Radiol* 2019;26(10):1338–44.
30. Taghipour M, Ziaei A, Alessandrino F, Hassanzadeh E, Harisinghani M, Vangel M, et al. Investigating the role of DCE-MRI, over T2 and DWI, in accurate PI-RADS v2 assessment of clinically significant peripheral zone prostate lesions as defined at radical prostatectomy. *Abdom Radiol (New York)* 2018;44(4):1520–7.
31. Gatti M, Faletti R, Callaris G, Giglio J, Berzovini C, Gen tile F, et al. Prostate cancer detection with biparametric magnetic resonance imaging (bpMRI) by readers with different experience: performance and comparison with multiparametric (mpMRI). *Abdom Radiol (New York)* 2019;44(5):1883–93.